Title

Elevated PSD-95 Blocks Ion-flux Independent LTD: A Potential New Role for PSD-95 in Synaptic Plasticity

Authors

Dore, Kim
Malinow, Roberto

Publication Date

2021-02-01

DOI

10.1016/j.neuroscience.2020.02.020

Peer reviewed

HHS Public Access

Author manuscript

Neuroscience. Author manuscript; available in PMC 2022 February 21.

Published in final edited form as:

Neuroscience. 2021 February 21; 456: 43–49. doi:10.1016/j.neuroscience.2020.02.020.

Elevated PSD-95 blocks ion-flux independent LTD: a potential new role for PSD-95 in synaptic plasticity

Kim Dore[1,*], **Roberto Malinow**[1]

[1]Center for Neural Circuits and Behavior, Department of Neuroscience and Section for Neurobiology, Division of Biology, University of California at San Diego, San Diego, CA 92093.

Abstract

We recently demonstrated that NMDA receptors (NMDARs) are capable of ion-flux independent signaling through conformational change in the NMDAR intracellular domain resulting in long-term depression of synaptic transmission (LTD). Here we show that PSD-95 overexpression blocks agonist induced conformational movement in the NMDAR intracellular domain as well as LTD that is NMDAR-dependent and ion-flux independent. Interestingly, previous studies indicate that overexpressed PSD-95 does not block NMDAR-dependent LTD. These data support a model where ion-flux independent LTD is predominant in young animals, which have synapses with low amounts of PSD-95, whereas only ion flux dependent LTD occurs at more mature synapses, which have more PSD-95 that would block ion-flux independent LTD. These results may reconcile different findings regarding ion-flux independent LTD.

Keywords

Long-term depression; NMDA receptor; metabotropic signaling; conformational movement; post-synaptic density protein 95; MAGUK

Introduction

The NMDAR is an important member of the ionotropic glutamate receptor family required for both long-term potentiation (LTP) and depression (LTD) of synaptic transmission (Traynelis et al., 2010). We have shown that low-frequency stimulation (LFS) produces NMDAR-dependent LTD in the presence of two antagonists that can effectively block ion-flux through the NMDAR (MK-801 or 7-chloro-kynurenate) (Nabavi et al., 2013). We have also used FRET-FLIM to demonstrate that glutamate or NMDA binding can induce a conformational movement in the NMDAR carboxyl(c)-terminal domain that is independent of ion-flux and triggers downstream events leading to LTD (Dore et al., 2015). These

*Correspondence to: K.D., kdore@ucsd.edu.

Disclosure Statement

The authors declare no competing financial interests.

findings are in disagreement with the long-standing model stating that LTD requires a moderate rise in cytoplasmic Ca^{2+} (Malenka, 1994, Lisman, 1989), making this ion-flux-independent mechanism for NMDAR-dependent LTD controversial (Babiec et al., 2014; Sanderson et al., 2016; Volianskis et al., 2015). However, some recent studies have confirmed our findings (Carter and Jahr, 2016; Stein et al., 2015; Wong and Gray, 2018), implying that ion-flux dependent and independent mechanisms for NMDAR-dependent LTD might both exist. Moreover, several other studies reported ion-flux independent functions for other ligand-gated ion channels (reviewed in (Valbuena and Lerma, 2016) and even voltage-gated ion channels (Kaczmarek, 2006); suggesting that these channels are more polyvalent than we originally thought.

Another unresolved aspect about LTD is how the scaffolding protein PSD-95 is affecting this form of synaptic plasticity. While PSD-95 overexpression enhance LTD (Beique et al., 2006; Ehrlich and Malinow, 2004; Stein et al., 2003), LTD in animals older than 3-weeks (in which PSD-95 levels are maximal (Chang et al., 2009; Zhu et al., 2011)) is reduced (Dudek and Bear, 1993) or completely absent (Wagner and Alger, 1995). Since PSD-95 promotes the synaptic insertion of AMPA receptors (Ehrlich and Malinow, 2004), which potentiates synaptic transmission and occludes LTP (Beique et al., 2006; Ehrlich and Malinow, 2004), it make sense that ion-flux dependent LTD, which removes AMPA receptors, is enhanced by PSD-95 overexpression. However, PSD-95 directly interacts with the NMDAR c-terminal domain (Dore et al., 2014; Kornau et al., 1995), which could block conformational movement in this intracellular domain and thus ion-flux independent LTD. This suggests that PSD-95 might affect ion-flux dependent and ion-flux independent LTD differently.

Here we examine the impact of overexpressed PSD-95 on these two forms of plasticity. Surprisingly, we find that elevated PSD-95 blocks ion-flux independent LTD. We also confirm that elevated PSD-95 does not block LTD if ion-flux is permitted. It is notable that most experiments failing to observe ion-flux independent LTD have used mice (Babiec et al., 2014; Sanderson et al., 2016), which display elevated PSD-95 earlier in development compared to rats (Chang et al., 2009; Ling et al., 2012; Zheng et al., 2012; Zhu et al., 2011). It may be that differences in synaptic PSD-95 could account for different experimental findings. Furthermore, we propose that ion-flux independent LTD is present only when synaptic PSD-95 levels are low such as early in development (when synapses with only NMDAR (Isaac et al., 1995; Liao et al., 1995) are more prevalent (Isaac et al., 1997; Wu et al., 1996), and ion-flux would be expected to be minimal) or in disease.

Experimental Procedures

Primary hippocampal neurons and organotypic hippocampal slices

Primary hippocampal neurons from P0-P1 Sprague-Dawley rat pups (Envigo) were made as previously described (Dore et al., 2015) with minor modifications. Briefly, GS21 (GlobalStem) was used instead of B-27, neurons were plated as a single 300μl ~10^6 cells/mL drop onto 18mm glass coverslips (Neuvitro) and cytosine arabinoside was omitted to improve neuronal health. Cultures were transfected at 7-10 days in vitro (DIV) with GluN1-GFP, GluN2B and GluN1-mCherry (GluN1-mCherry was omitted in some samples in order to measure FRET efficiency, see below) as in (Dore et al., 2015) and imaged at 14-16DIV.

Organotypic hippocampal slices were prepared from P6-7 Sprague-Dawley rat pups as described previously (Shi et al., 1999) and used at 6–10 DIV. The CA3 region was surgically removed in organotypic slices to prevent stimulus-induced bursting. 18-24h before using primary cultures or organotypic slices; preparations were infected with a Sindbis virus expressing nuclear localized mCherry (NLS-mCherry, pSR5-NLS-mCherry) or pSR5-NLS-mCherry-T2A-PSD95. Infection of neurons with this PSD-95 expressing virus resulted in a 3-fold increase of PSD-95 levels in spines of primary neurons and 1.7-fold in organotypic slices. All procedures involving animals were approved by the Institutional Animal Care and Use Committees of the University of California, San Diego.

Fluorescence lifetime imaging

Fluorescence lifetime imaging was performed as previously described (Dore et al., 2015). Briefly, a SliceScope two-photon microscope (Scientifica, UK) equipped with a 60X water immersion objective (LUMPLFLN 60XW, NA = 1.0, Olympus), a hybrid PMT detector (HPM-100-40, Becker and Hickl, Germany) and a TCSPC module (SPC-150, Becker and Hickl). A Chameleon Ultra II IR laser (Coherent) (80 MHz repetition rate, 100–150 fs pulses) tuned at 930nm was used for the excitation of GluN1-GFP. ScanImage r3.8 was used to control the scanning mirrors (Pologruto et al., 2003). Neurons were imaged in a circulating Hank's balanced salt solution (HBSS) containing 0.3mM $CaCl_2$, 5mM $MgCl_2$ and 100μM of 7CK (Tocris). A baseline image was first acquired in that solution, then 25μM NMDA was added and the same neurons were imaged a second time. Fluorescence lifetime images were analyzed using SPCImage (Becker et al., 2004); with a binning factor of 6-10 and a minimum threshold of 10 photons at the peak time bin. A custom Matlab program was used to select dendritic spines and extract one mean fluorescence lifetime value per spine; the same regions of interest (ROIs) were used to measure the effect of NMDA application in the same neurons (See (Dore et al., 2015) for more details). To calculate FRET efficiency the following formula was used: $EFRET= 1-T_{DA}/T_D$ (T_{DA} = lifetime of the donor in the presence of the acceptor, T_D = average lifetime of the donor alone) (Lakowicz, 2006).

Electrophysiology

Recordings of organotypic slices were performed in a continuous flow of oxygenated artificial cerebrospinal fluid (ACSF), containing 119mM NaCl, 2.5mM KCl, 26mM $NaHCO_3$, 1mM NaH_2PO_4, 11mM glucose, 100μM gabazine, 2mM $CaCl_2$, 2mM $MgCl_2$, and 4μM 2-chloroadenosine, 10μM of L689,560 was added where indicated (pH 7.4). All experiments were performed at 24–28°C. Whole-cell recordings were obtained from individual cells in CA1 region using glass pipettes (3–5 MΩ) filled with a cesium methanesulfonate internal solution containing, in mM: 115 cesium methanesulfonate, 20 CsCl, 10 FIEPES, 2.5 $MgCl_2$, 4 Na_2ATP, 0.4 Na_3GTP, 10 sodium phosphocreatine, 0.6 EGTA, and 0.1 spermine, pH 7.25). Synaptic responses were evoked by stimulating two independent pathways using bipolar stimulating electrodes (Frederick Haer) placed 150–250μm down the apical dendrites, 100μm apart, and 150–200μm laterally in opposite directions. After 20-min baseline, established by stimulating two independent pathways at 0.1 Hz, LTD was induced in one pathway by applying 900 pulses at 1Hz. Experiments were excluded if series resistance increased by more than 30%.

PSD-95 expression time course in rats and mice

In Fig. 4 we evaluated PSD-95 expression levels in rats and mice of different ages. P7, P14, P21, P28 and P35 Sprague-Dawley rats were obtained from Envigo as described above, C57BL/6 mice of the same ages were obtained from Jackson laboratories (stock #000664). One animal per age was processed for this experiment. One hemi-brain was fixed in 4% paraformaldehyde for 48h and was subsequently sliced on a vibratome for immunofluorescence experiments; the other hemi-brain was flash frozen and used for biochemical quantification.

Quantification of PSD-95 levels with immunofluorescence (Fig. 4AB): 2 separate 50μm slices per animal slices were first permeabilized and blocked with a solution containing 0.2% TritonX-100 and 3% normal goat serum for one hour at room temperature. Slices were then labeled with a PSD-95 antibody (MA1-046, ThermoFisher), 1/500 dilution, overnight at 4°C; a goat anti-mouse secondary antibody (GAM-AF568, Life Technologies) was used the next day at a 1/1000 dilution. After xylene clearing, samples were mounted in Krystalon mounting media and imaged using a FV1000 confocal microscope. The CA1 region of the hippocampus was imaged in each slice (3 images/slice) and PSD-95 levels were measured blindly with Fiji (ImageJ).

Quantification of PSD-95 levels with biochemistry (Fig. 4C): cerebrums were dissected from frozen hemi-brains and cut into small pieces with a scalpel. Each cerebrum was then homogenized with mechanical trituration and a Sonica ultrasonic processor in ice-cold RIPA buffer (50mM Tris HCl, PH 7.4, 150mM NaCl, 1% Triton X-100, 0.5% Sodium deoxylcholate, 0.1% SDS, 1mM EDTA, 10mM NaF, 1mM PMSF). After a 10 minutes 10000g centrifugation, supernatants from each brain were divided in 3 samples and protein concentration was determined with the BCA assay (Pierce) and normalized. Samples of equivalent amounts of protein were then ran on 4-20% Tris-Glycine gels (Bio-Rad). After transfer onto PDVF membranes (Bio-Rad), blotting was carried on overnight at 4°C against PSD-95 (MA1-046, Thermofisher) and actin (Cell Signaling Technologies, #3700) at 1/1000 dilution in 5% milk in TBS-T. Blots were then incubated with a HRP-conjugated goat anti-mouse secondary antibody (Cell Signaling Technologies, #7076), 1/1000 dilution in 5% milk in TBS-T for 1h at room temperature. Pierce ECL was used for chemiluminescence; immunoblots were then visualized with a Bio-Rad imager and analyzed using ImageJ.

Results

PSD-95 overexpression blocks NMDA-induced conformational movement in the NMDAR c-terminal domain

To test the effect of PSD-95 overexpression on the NMDAR metabotropic function, we co-expressed recombinant GluN1 subunits of the NMDAR tagged with GFP or mCherry at their c-terminus; 24h before imaging neurons were infected with a Sindbis virus expressing nuclear localized mCherry (NLS-mCherry) with or without PSD-95 (Fig. 1AB). Since GluN1 constructs are excluded from the nucleus, this method permitted the identification of neurons expressing both the GluN1 subunits as well as the Sindbis virus. Neurons were then imaged in the presence of 7-chloro-kynurenate (7CK) with a two-photon microscope

capable of measuring GFP fluorescence lifetime. Since the fluorescence lifetime of GluN1-GFP, the FRET donor, is highly sensitive to the proximity of GluN1-mCherry, the FRET acceptor; fluorescence lifetime imaging microscopy (FLIM) can be used measure Forster resonance energy transfer (FRET) in a precise and quantitative manner (Dore et al., 2015; Yasuda, 2006). FRET efficiency was measured by comparing neurons expressing GluN1-GFP/GluN1-mCherry to neurons expressing only GluN1-GFP in the same conditions (see Experimental Procedures). Interestingly, PSD-95 overexpression did not affect basal NMDAR FRET efficiency, suggesting that increased NMDAR-PSD95 interactions had little effect on baseline NMDAR conformation. The same neurons were then imaged a second time after the addition of 25μM NMDA (a stimulus that produces long-term depression of synaptic transmission, cLTD (Aow et al., 2015). As expected, cLTD induced an increase in fluorescence lifetime and a decrease in FRET efficiency in control neurons expressing NLS-mCherry. However, this change in FRET was blocked in neurons overexpressing PSD-95 (Fig. 1CD).

PSD-95 overexpression selectively blocks ion-flux independent LTD

To see how blockade of NMDAR c-terminal movement by PSD-95 overexpression affects electrically induced LTD, we performed whole-cell recordings in organotypic hippocampal slices infected or not with NLS-mCherry + PSD-95. Since 7CK affects AMPA receptor mediated transmission (Nabavi et al., 2013; Wong and Gray, 2018), we used L689,560 (L689) which blocks NMDAR at the glycine binding site as effectively as 7CK but minimally affects AMPA receptor-mediated EPSCs (Wong and Gray, 2018). Initially we confirmed this by measuring excitatory post-synaptic currents (EPSCs) at different holding potentials, with and without L689. AMPA receptor mediated responses were first recorded at −60mV, NMDAR currents were then measured at +40mV, and L689 was added to the perfusion. Five minutes later, NMDAR mediated responses at +40mV were completely blocked while responses at −60mV were unaffected (Fig. 2AB). To examine LTD in the presence of L689, we recorded EPSCs at −60mV using two stimulating electrodes producing two independent pathways. In uninfected neurons, after a 20-minute baseline, a 15-minute 1Hz stimulation protocol induced LTD in the stimulated pathway, whereas the control pathway remained at baseline levels (Fig. 2C). This result is consistent with data obtained using acute slices (Nabavi et al., 2013; Wong and Gray, 2018). However, quite strikingly, ion-flux independent LTD was completely blocked in neurons overexpressing PSD-95 (Fig. 2DE).

To assess how PSD-95 overexpression affects ion-flux dependent LTD in the same experimental conditions, we repeated the LTD recordings in the absence of L689. Figure 3 shows that similarly to what was previously reported (Beique et al., 2006; Stein et al., 2003), PSD-95 overexpression does not block ion-flux dependent LTD and contrary to its effect on ion-flux independent LTD, appears to slightly facilitate LTD.

Previous studies examining ion-flux independent LTD have used mice and rats of different ages. We wished to test if the different results might be explained by differences in endogenous PSD-95 with age, and in species (see (Chang et al., 2009; Ling et al., 2012; Zheng et al., 2012; Zhu et al., 2011). Since these studies did not compare PSD-95 levels in

rats and mice at the same time and across the whole developmental period for both species, we decided to carefully evaluate this important characteristic. As seen in Fig. 4AB, PSD-95 expression levels in the CA1 region of the hippocampus (exactly where LTD experiments are done) are maximal in 21-days old mice and are still increasing in 35-days rats. Similar results were obtained by biochemical analysis of mice and rat cerebrums (Fig. 4C).

Discussion

In this study, we investigated the role of PSD-95 levels on ion-flux independent LTD. We find that overexpressing this important structural protein blocks this form of synaptic plasticity. In agreement with conformational movement in the NMDAR c-terminal domain being required for this form of LTD (Aow et al., 2015), we find that overexpression of PSD-95 also blocks this conformational movement. Notably, we confirm that overexpression of PSD-95 does not block NMDAR-dependent LTD when ion-flux is permitted (Beique et al., 2006; Stein et al., 2003). Thus, elevated levels of PSD-95 differentially affect these two forms of LTD.

Because PSD-95 levels are dramatically changing during development, elevated PSD-95 could be a way to limit synaptic depression in mature synapses. Moreover, since PSD-95 levels appears to peak earlier in mice (around P21, Fig. 4) than in rats (still not maximal at P35 (Fig. 4); this could explain why some laboratories were not able to observe ion-flux independent LTD. Both recent studies reporting that MK801 blocked LTD (Babiec et al., 2014; Sanderson et al., 2016) used mice (8-12 weeks, P14-21 and P18-21). Given our results showing a large change in PSD-95 between P14 and P21, it will be important to repeat such studies with exact mouse ages reported. The Collingridge laboratory reported that L689 blocked LTD in 14-days old rats (Volianskis et al., 2015). However, a control pathway was not included and L689 was washed in and out of the perfusion in these experiments, both of which complicate studying this form of plasticity (Nabavi et al., 2014).

Ion-flux independent LTD may be more prevalent in immature synapses, which contain more synapses with only NMDAR and no AMPARs (Isaac et al., 1997; Wu et al., 1996). Such synapses, if activated alone, would be expected to produce minimal ion-flux. Ion-flux independent LTD in immature synapses could be a way to enhance spine pruning, an essential mechanism that decreases when the brain matures (Holtmaat and Svoboda, 2009). Moreover, ion-flux independent NMDAR function has been implicated in beta-amyloid induced depression (Birnbaum et al., 2015; Kessels et al., 2013; Tamburri et al., 2013). Interestingly, beta-amyloid decreases PSD-95 levels in synapses (Almeida et al., 2005). PSD-95 levels are also reduced in several mouse models of Alzheimer’s disease (Hong et al., 2016; Shao et al., 2011) as well as in human patients with the disease (Gylys et al., 2004; Proctor et al., 2010). Moreover, it was also reported that synaptic PSD-95 levels were reduced in a model of Parkinson’s disease (Nash et al., 2005). Our findings thus suggest that immature or diseased synapses would be more sensitive to ion-flux independent LTD. In conclusion, we find elevated PSD-95 blocks ion-flux independent LTD, and this may reconcile conflicting LTD studies.

Acknowledgments

This work was supported by the NIH (R01-MH049159) to R.M. Confocal microscopy shown in Figure 4 was done at UCSD Microscopy School of Medicine CORE facility (NINDS Core Grant NS047101).

References

Almeida CG, Tampellini D, Takahashi RH, Greengard P, Lin MT, Snyder EM, and Gouras GK (2005). Beta-amyloid accumulation in APP mutant neurons reduces PSD-95 and GluR1 in synapses. Neurobiology of disease 20, 187–198. [PubMed: 16242627]

Aow J, Dore K, and Malinow R (2015). Conformational signaling required for synaptic plasticity by the NMDA receptor complex. Proceedings of the National Academy of Sciences of the United States of America 112, 14711–14716. [PubMed: 26553983]

Babiec WE, Guglietta R, Jami SA, Morishita W, Malenka RC, and O'Dell TJ (2014). Ionotropic NMDA receptor signaling is required for the induction of long-term depression in the mouse hippocampal CA1 region. The Journal of neuroscience : the official journal of the Society for Neuroscience 34, 5285–5290. [PubMed: 24719106]

Becker W, Bergmann A, Hink MA, Konig K, Benndorf K, and Biskup C (2004). Fluorescence lifetime imaging by time-correlated single-photon counting. Microscopy Research and Technique 63, 58–66. [PubMed: 14677134]

Beique JC, Lin DT, Kang MG, Aizawa H, Takamiya K, and Huganir RL (2006). Synapse-specific regulation of AMPA receptor function by PSD-95. Proceedings of the National Academy of Sciences of the United States of America 103, 19535–19540. [PubMed: 17148601]

Birnbaum JH, Bali J, Rajendran L, Nitsch RM, and Tackenberg C (2015). Calcium flux-independent NMDA receptor activity is required for A beta oligomer-induced synaptic loss. Cell Death Dis 6.

Carter BC, and Jahr CE (2016). Postsynaptic, not presynaptic NMDA receptors are required for spike-timing-dependent LTD induction. Nature neuroscience.

Chang LR, Liu JP, Zhang N, Wang YJ, Gao XL, and Wu Y (2009). Different expression of NR2B and PSD-95 in rat hippocampal subregions during postnatal development. Microsc Res Tech 72, 517–524. [PubMed: 19306263]

Dore K, Aow J, and Malinow R (2015). Agonist binding to the NMDA receptor drives movement of its cytoplasmic domain without ion flow. Proceedings of the National Academy of Sciences of the United States of America 112, 14705–14710. [PubMed: 26553997]

Dore K, Labrecque S, Tardif C, and De Koninck P (2014). FRET-FLIM investigation of PSD95-NMDA receptor interaction in dendritic spines; control by calpain, CaMKII and Src family kinase. PloS one 9, e112170. [PubMed: 25393018]

Dudek SM, and Bear MF (1993). Bidirectional long-term modification of synaptic effectiveness in the adult and immature hippocampus. The Journal of neuroscience : the official journal of the Society for Neuroscience 13, 2910–2918. [PubMed: 8331379]

Ehrlich I, and Malinow R (2004). Postsynaptic density 95 controls AMPA receptor incorporation during long-term potentiation and experience-driven synaptic plasticity. The Journal of neuroscience : the official journal of the Society for Neuroscience 24, 916–927. [PubMed: 14749436]

Gylys KH, Fein JA, Yang F, Wiley DJ, Miller CA, and Cole GM (2004). Synaptic changes in Alzheimer's disease: increased amyloid-beta and gliosis in surviving terminals is accompanied by decreased PSD-95 fluorescence. Am J Pathol 165, 1809–1817. [PubMed: 15509549]

Holtmaat A, and Svoboda K (2009). Experience-dependent structural synaptic plasticity in the mammalian brain. Nature reviews Neuroscience 10, 647–658. [PubMed: 19693029]

Hong S, Beja-Glasser VF, Nfonoyim BM, Frouin A, Li S, Ramakrishnan S, Merry KM, Shi Q, Rosenthal A, Barres BA, et al. (2016). Complement and microglia mediate early synapse loss in Alzheimer mouse models. Science 352, 712–716. [PubMed: 27033548]

Isaac JT, Crair MC, Nicoll RA, and Malenka RC (1997). Silent synapses during development of thalamocortical inputs. Neuron 18, 269–280. [PubMed: 9052797]

Isaac JT, Nicoll RA, and Malenka RC (1995). Evidence for silent synapses: implications for the expression of LTP. Neuron 15, 427–434. [PubMed: 7646894]

Kaczmarek LK (2006). Non-conducting functions of voltage-gated ion channels. Nature reviews Neuroscience 7, 761–771. [PubMed: 16988652]

Kessels HW, Nabavi S, and Malinow R (2013). Metabotropic NMDA receptor function is required for beta-amyloid-induced synaptic depression. Proceedings of the National Academy of Sciences of the United States of America 110, 4033–4038. [PubMed: 23431156]

Kornau HC, Schenker LT, Kennedy MB, and Seeburg PH (1995). Domain interaction between NMDA receptor subunits and the postsynaptic density protein PSD-95. Science 269, 1737–1740. [PubMed: 7569905]

Lakowicz JR (2006). Principles of fluorescence spectrocopy, 3rd Edition (Spinger).

Liao D, Hessler NA, and Malinow R (1995). Activation of postsynaptically silent synapses during pairing-induced LTP in CA1 region of hippocampal slice. Nature 375, 400–404. [PubMed: 7760933]

Ling W, Chang L, Song Y, Lu T, Jiang Y, Li Y, and Wu Y (2012). Immunolocalization of NR1, NR2A, and PSD-95 in rat hippocampal subregions during postnatal development. Acta Histochem 114, 285–295. [PubMed: 21719075]

Nabavi S, Fox R, Alfonso S, Aow J, and Malinow R (2014). GluA1 trafficking and metabotropic NMDA: addressing results from other laboratories inconsistent with ours. Philosophical transactions of the Royal Society of London Series B, Biological sciences 369, 20130145. [PubMed: 24298147]

Nabavi S, Kessels HW, Alfonso S, Aow J, Fox R, and Malinow R (2013). Metabotropic NMDA receptor function is required for NMDA receptor-dependent long-term depression. Proceedings of the National Academy of Sciences of the United States of America 110, 4027–4032. [PubMed: 23431133]

Nash JE, Johnston TH, Collingridge GL, Garner CC, and Brotchie JM (2005). Subcellular redistribution of the synapse-associated proteins PSD-95 and SAP97 in animal models of Parkinson's disease and L-DOPA-induced dyskinesia. FASEB journal : official publication of the Federation of American Societies for Experimental Biology 19, 583–585. [PubMed: 15703272]

Pologruto TA, Sabatini BL, and Svoboda K (2003). ScanImage: flexible software for operating laser scanning microscopes. Biomed Eng Online 2, 13. [PubMed: 12801419]

Proctor DT, Coulson EJ, and Dodd PR (2010). Reduction in post-synaptic scaffolding PSD-95 and SAP-102 protein levels in the Alzheimer inferior temporal cortex is correlated with disease pathology. J Alzheimers Dis 21, 795–811. [PubMed: 20634587]

Sanderson JL, Gorski JA, and Dell'Acqua ML (2016). NMDA Receptor-Dependent LTD Requires Transient Synaptic Incorporation of Ca(2+)-Permeable AMPARs Mediated by AKAP150-Anchored PKA and Calcineurin. Neuron 89, 1000–1015. [PubMed: 26938443]

Shao CY, Mirra SS, Sait HB, Sacktor TC, and Sigurdsson EM (2011). Postsynaptic degeneration as revealed by PSD-95 reduction occurs after advanced Abeta and tau pathology in transgenic mouse models of Alzheimer's disease. Acta Neuropathol 122, 285–292. [PubMed: 21630115]

Shi SH, Hayashi Y, Petralia RS, Zaman SH, Wenthold RJ, Svoboda K, and Malinow R (1999). Rapid spine delivery and redistribution of AMPA receptors after synaptic NMDA receptor activation. Science 284, 1811–1816. [PubMed: 10364548]

Stein IS, Gray JA, and Zito K (2015). Non-Ionotropic NMDA Receptor Signaling Drives Activity-Induced Dendritic Spine Shrinkage. The Journal of neuroscience : the official journal of the Society for Neuroscience 35, 12303–12308. [PubMed: 26338340]

Stein V, House DR, Bredt DS, and Nicoll RA (2003). Postsynaptic density-95 mimics and occludes hippocampal long-term potentiation and enhances long-term depression. The Journal of neuroscience : the official journal of the Society for Neuroscience 23, 5503–5506. [PubMed: 12843250]

Tamburri A, Dudilot A, Licea S, Bourgeois C, and Boehm J (2013). NMDA-receptor activation but not ion flux is required for amyloid-beta induced synaptic depression. PloS one 8, e65350. [PubMed: 23750255]

Traynelis SF, Wollmuth LP, McBain CJ, Menniti FS, Vance KM, Ogden KK, Hansen KB, Yuan H, Myers SJ, and Dingledine R (2010). Glutamate receptor ion channels: structure, regulation, and function. Pharmacological reviews 62, 405–496. [PubMed: 20716669]

Valbuena S, and Lerma J (2016). Non-canonical Signaling, the Flidden Life of Ligand-Gated Ion Channels. Neuron 92, 316–329. [PubMed: 27764665]

Volianskis A, France G, Jensen MS, Bortolotto ZA, Jane DE, and Collingridge GL (2015). Long-term potentiation and the role of N-methyl-D-aspartate receptors. Brain research 1621, 5–16. [PubMed: 25619552]

Wagner JJ, and Alger BE (1995). GABAergic and developmental influences on homosynaptic LTD and depotentiation in rat hippocampus. The Journal of neuroscience : the official journal of the Society for Neuroscience 15, 1577–1586. [PubMed: 7869119]

Wong JM, and Gray JA (2018). Long-Term Depression Is Independent of GluN2 Subunit Composition. The Journal of neuroscience : the official journal of the Society for Neuroscience 38, 4462–4470. [PubMed: 29593052]

Wu G, Malinow R, and Cline HT (1996). Maturation of a central glutamatergic synapse. Science 274, 972–976. [PubMed: 8875937]

Yasuda R (2006). Imaging spatiotemporal dynamics of neuronal signaling using fluorescence resonance energy transfer and fluorescence lifetime imaging microscopy. Current opinion in neurobiology 16, 551–561. [PubMed: 16971112]

Zheng S, Gray EE, Chawla G, Porse BT, O'Dell TJ, and Black DL (2012). PSD-95 is post-transcriptionally repressed during early neural development by PTBP1 and PTBP2. Nature neuroscience 15, 381–388, S381. [PubMed: 22246437]

Zhu ZW, Xu Q, Zhao ZY, Gu WZ, and Wu DW (2011). Spatiotemporal expression of PSD-95 in Fmr1 knockout mice brain. Neuropathology 31, 223–229. [PubMed: 21092061]

Highlights

- PSD-95 overexpression blocks NMDA receptor dependent ion-flux independent LTD.
- This property distinguishes ion-flux dependent and independent forms of LTD.
- Ion-flux independent LTD could enhance pruning in synapses with less PSD-95.
- Different PSD-95 expression in mice and rats may reconcile conflicting LTD studies.

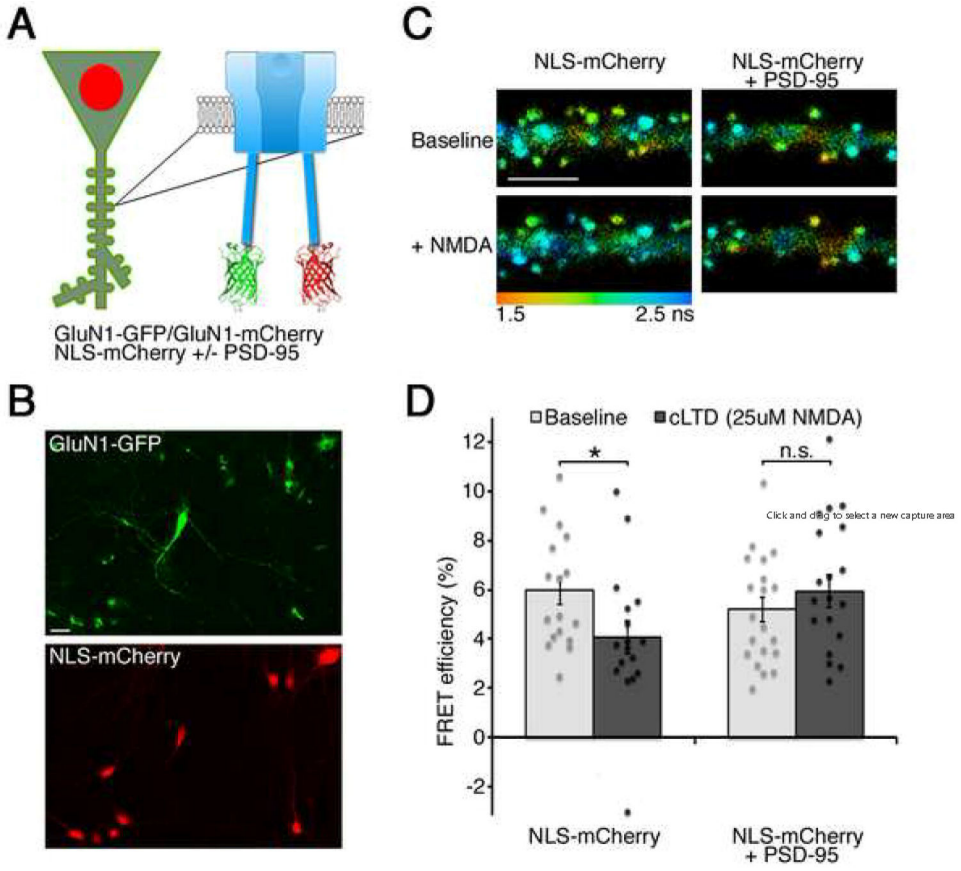

Figure 1: PSD-95 overexpression blocks NMDA-induced conformational movement in the NMDAR c-terminal domain

A) Experimental design.

B) Field of neurons transfected with GluN1-GFP and infected with Sindbis expressing nuclear localization signal tagged (NLS)-mCherry. Scale bar, 20μm

C) (*Top*) Representative images of neurons expressing GluN1-GFP/GluN1-mCherry and NLS-mCherry or NLS-mCherry + PSD-95 in a solution containing 100μM 7CK, (*Bottom*) same neurons in the presence of 100μM 7CK and 25μM NMDA. Pseudo-colored pixels indicating fluorescence lifetime of GluN1-GFP (see color scale); scale bar, 5μm.

D) Average FRET efficiency for the indicated conditions; N>17 neurons per condition, individual data points for each neuron are superimposed; *p<0.05, paired *t*-test.

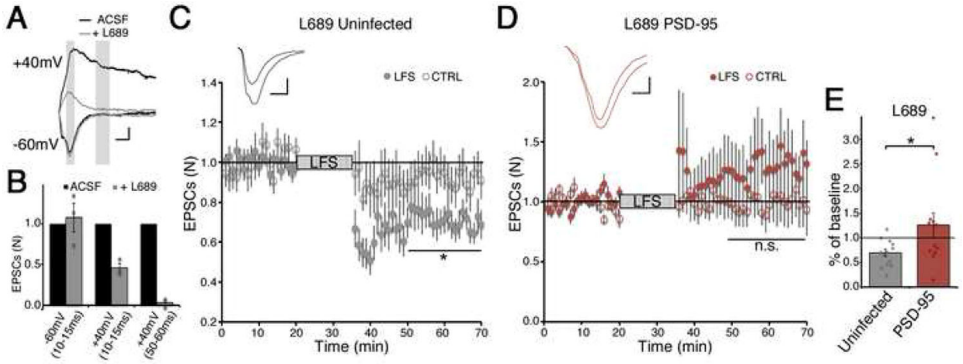

Figure 2: PSD-95 overexpression blocks ion-flux independent LTD

A) Representative EPSCs obtained at −60 or +40mV in normal ACSF (black) or in the presence of 10μM L689 (gray). Shaded areas are analyzed in B. Scale bars, 10ms, 20pA throughout.

B) Effect of L689 on EPSCs recorded at −60 or +40mV at peak amplitude (10-15ms after stimulation) or at 50-60ms when only NMDAR currents are observed. N=3.

C) Whole-cell LTD recordings from two independent pathways in 10μM L689 in uninfected CA1 neurons; one pathway (filled symbols) received a 15-min 1-Hz low frequency stimulus (LFS), where indicated. The control pathway (open circles) received no stimulus. (*Inset*) Representative responses obtained before and after LFS. Error bars represent SEM, N=13. *p<0.05, paired *t*-test.

D) As in C) but in neurons expressing NLS-mCherry + PSD-95. LFS produces no depression. N=13.

E) PSD-95 overexpression blocks LFS-induced LTD in the presence of L689. Individual data points for each neuron are superimposed; N=13. *p< 0.05, unpaired *t*-test.

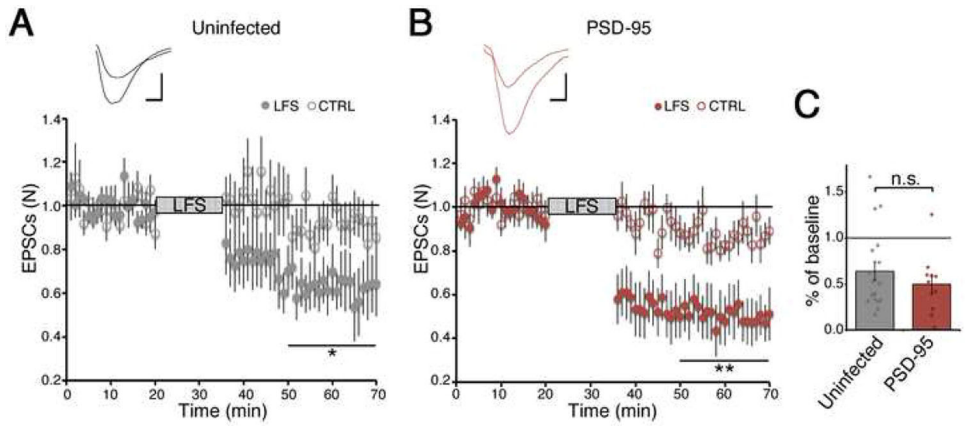

Figure 3: PSD-95 overexpression does not block ion-flux dependent LTD

A) Whole-cell LTD recordings from two independent pathways in uninfected CA1 neurons; one pathway (filled symbols) received LFS, where indicated. The control pathway (open circles) received no stimulus. Error bars represent SEM, N=17, *p<0.05, paired *t*-test. (*Inset*) Representative responses obtained before and after LFS. Scale bars, 10ms, 10pA.

B) As in A) but in neurons expressing NLS-mCherry + PSD-95. N=10; **p<0.01, paired *t*-test.

C) PSD-95 overexpression does not significantly affect LFS-induced LTD. N>10, individual data points for each neuron are superimposed, non-significant (n.s.), unpaired *t*-test.

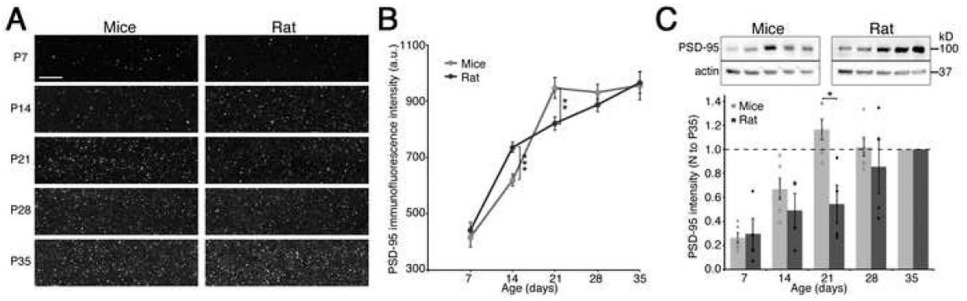

Figure 4: PSD-95 expression levels in mice and rats

A) Representative immunofluorescence images of PSD-95 levels in the CA1 region of the hippocampus of mice and rats of indicated ages. Scale bar is 10μm.

B) Quantification of PSD-95 immunofluorescence in animals of indicated ages. N = 2 slices/animal, 3 images/slice, 5 ROIs/image; **p<0.01, ***p<0.001; unpaired *t*-test.

C) Representative immunoblots of PSD-95 and actin in mice and rat cerebrum. PSD-95 band was normalized by the corresponding actin band and this ratio was then normalized to P35 signal. N=4 (rats) N=6 (mice), individual data points for each experiment are superimposed; *p<0.05; unpaired *t*-test.